Phospholipase C-mediated calcium signalling is required for fungal development and pathogenicity in *Magnaporthe oryzae*

HEE-SOOL RHO, JUNHYUN JEON AND YONG-HWAN LEE

Department of Agricultural Biotechnology, Center for Fungal Pathogenesis, and Center for Fungal Genetic Resources, Seoul National University, Seoul 151-921, Korea

SUMMARY

Calcium signalling has profound implications in the fungal infection of plants and animals, during which a series of physiological and morphological transitions are required. In this article, using a model fungal pathogen, *Magnaporthe oryzae*, we demonstrate that the regulation of the intracellular calcium concentration ($[Ca^{2+}]_{int}$) is essential for fungal development and pathogenesis. Imaging of $[Ca^{2+}]_{int}$ showed that infection-specific morphogenesis is highly correlated with the spatiotemporal regulation of calcium flux. Deletion of the fungal phospholipase C gene (*M. oryzae* phospholipase C 1, *MoPLC1*) suppressed calcium flux, resulting in a fungus defective in developmental steps, including appressorium formation and pathogenicity. Surprisingly, the *PLC-δ1* gene of mouse was able to functionally substitute for *MoPLC1* by restoring the calcium flux, suggesting the evolutionary conservation of the phospholipase C-mediated regulation of calcium flux. Our results reveal that MoPLC1 is a conserved modulator of calcium flux that is essential for the regulation of key steps in fungal development and pathogenesis.

INTRODUCTION

Fungal disease is a major cause of yield losses in crop plants and a rapid increase in systemic mycosis in immunocompromised individuals (Odds *et al.*, 2001; Sexton and Howlett, 2006). Successful fungal infection and colonization of the host require the spatial and temporal regulation of the physiology and morphology of cells in response to the host environment. In the light of this, an understanding of the signal transduction pathways that enable such regulation is of particular importance in order to decode the pathogenic mechanisms and evolution of fungi (Lengeler *et al.*, 2000). Signalling cascades operate throughout the entire infection process and do not vary greatly with the lifestyles of pathogens (Sexton and Howlett, 2006). Cyclic adenosine monophosphate (AMP)- and mitogen-activated protein (MAP)

kinase-dependent signalling cascades have been considerably well studied as the determinants of morphogenic events that lead to fungal infection (Idnurm *et al.*, 2005; Talbot, 2003). The involvement of Ca^{2+} signalling in fungal development has been suggested by either pharmacological approaches or imaging analysis. Studies using calcium chelators and other chemical treatments have suggested that fungi possess conserved components of the eukaryotic calcium signalling pathway, including calmodulin (Ahn *et al.*, 2003; Hoch *et al.*, 1987; Lee and Lee, 1998; Shaw and Hoch, 2000). Imaging analysis has revealed the presence of calcium gradients in fungal hyphae (Chandra *et al.*, 1999; Silverman-Gavrila and Lew, 2003). However, the genetic basis underlying the regulation of intracellular calcium concentration and its implication in fungal pathogenesis are poorly understood, despite the incredible versatility and universality of calcium signalling in eukaryotic cells (Berridge *et al.*, 1998, 2003).

Magnaporthe oryzae (Couch and Kohn, 2002) is a filamentous fungus that causes rice blast, the most devastating disease of cultivated rice (Zeigler *et al.*, 1994). The fungus is an important model in elucidating the pathogenic mechanisms of fungi because of its socioeconomic impact and genetic tractability (Jeon *et al.*, 2007). Recently, the availability of both rice and fungal genome sequences (Dean *et al.*, 2005; Goff *et al.*, 2002; Yu *et al.*, 2005) has provided a unique opportunity to study host–pathogen interactions at the genomic scale. As with most fungal pathogens, morphological transition plays an important role in host infection and colonization of the fungus. The infection of the host plant begins as a disseminated asexual spore, called a conidium, germinates in a water drop on a leaf surface. The germ tube apex, on recognizing the hydrophobicity of the contact surface, differentiates into a heavily melanized, dome-shaped infection structure, the appressorium (Lee and Dean, 1993, 1994). The fungus then gains entry into the plant cells by mechanical rupturing of the cuticular barrier of the plant using turgor pressure accumulated within the melanized appressorium (Howard *et al.*, 1991). Following penetration into plant tissues, the fungus develops bulbous invasive hyphae that are sealed in a plant membrane, and colonizes the host plant to form disease lesions over which it sporulates (Kankanala *et al.*, 2007).

* Correspondence: Tel.: +82 02 880 4674; Fax: +82 02 873 2317; E-mail: yonglee@snu.ac.kr

In this article, we describe the functional analysis of a fungal phosphoinositide-specific phospholipase C (PI-PLC) in *M. oryzae* (*M. oryzae* phospholipase C 1, MoPLC1). Imaging of the intracellular calcium concentration ($[Ca^{2+}]_{int}$) showed a clear association between induced calcium fluxes and infection-specific morphogenesis. Deletion of *MoPLC1* resulted in a fungus whose $[Ca^{2+}]_{int}$ did not respond to surface hydrophobicity. Analysis of an *MoPLC1* mutant indicated that MoPLC1-mediated calcium signalling is involved in an array of developmental processes. Surprisingly, the *PLC-δ1* gene of mouse was able to functionally substitute for *MoPLC1*. Our findings suggest that *MoPLC1* is an evolutionarily conserved modulator of calcium fluxes that regulates key steps in fungal pathogenesis.

RESULTS AND DISCUSSION

Intracellular calcium fluxes are implicated in surface sensing and infection-related morphogenesis of *M. oryzae*

Our previous study using a calcium chelator, ionophore and calmodulin antagonist suggested that the calcium-dependent signalling system is involved in appressorium formation of *M. oryzae* (Lee and Lee, 1998). In order to dissect the role of calcium ions in fungal pathogenesis, we monitored the relative $[Ca^{2+}]_{int}$ in germinating conidia of the wild-type strain 70-15 by imaging cells loaded with a calcium indicator (see Experimental procedures). When conidia were allowed to germinate on a hydrophobic surface, it was observed that $[Ca^{2+}]_{int}$ was elevated and localized initially at the site of germ tube emergence and at the tip of the elongating germ tube, and later within developing appressoria (Fig. 1A, top panels and bottom left panel). In contrast, germinating conidia on a hydrophilic surface, where the fungus rarely develops an appressorium, did not show localized calcium fluxes during prolonged elongation of the germ tube (Fig. 1A, bottom right panel), indicating that the calcium flux is induced by surface hydrophobicity and may therefore be involved in surface sensing. High $[Ca^{2+}]_{int}$ observed within developing appressoria suggests that calcium signalling plays a role in morphogenesis as well as surface sensing. However, the germination process appears to be independent of the calcium flux.

MoPLC1 encodes a PI-PLC-δ isoform that regulates intracellular calcium fluxes of *M. oryzae*

In eukaryotic cells, the release of concentrated organellar calcium into the cytoplasm is known to be regulated by PI-PLC, which hydrolyses a minor membrane phospholipid, phosphatidylinositol 4,5-bisphosphate (PIP$_2$), to produce inositol-1,4,5-triphosphate (IP$_3$) and diacylglycerol (DAG) (Rhee and Bae, 1997). The addition of neomycin, an inhibitor of phospholipase C (PLC), to *M. oryzae*
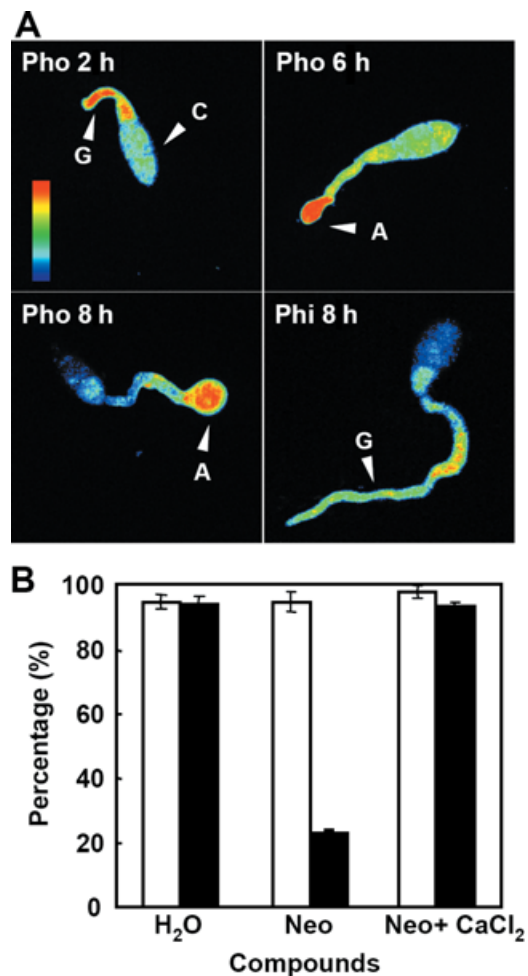

Fig. 1 Effects of *Magnaporthe oryzae* phospholipase C 1 (MoPLC1)-mediated calcium fluxes on fungal development. (A) Calcium fluxes within germinating conidia on a hydrophobic surface (Pho) and a hydrophilic surface (Phi) at 2, 6 and 8 h post-incubation. A, appressorium; C, conidium; G, germ tube. Coloured bars indicate the relative abundance of intracellular calcium ions ranging from the lowest (blue) to the highest (red). (B) Effect of a phospholipase C inhibitor, neomycin (Neo), on calcium fluxes and appressorium formation on a hydrophobic surface, and its complementation by exogenous calcium. The germination and appressorium formation of wild-type conidia on a hydrophobic surface compared between control (H$_2$O), neomycin treatment and addition of calcium chloride to conidial suspension following neomycin treatment. Open and filled bars indicate the percentage ratio of germinating conidia to total conidia counted and appressoria to germinating conidia, respectively.

conidial suspension suppressed the calcium fluxes at the germ tube apex and appressorium formation, even on a hydrophobic surface (Fig. 1B). This lack of calcium flux and fungal morphogenesis is reminiscent of the responses observed on a hydrophilic surface. The marked reduction in appressorium formation from conidia treated with neomycin could be restored by an external supply of

calcium ions (Fig. 1B). Our data suggest that appressorium formation requires calcium flux that is regulated by PLC.

The implication of PLC in the regulation of calcium flux, inferred from an analysis combining imaging technology and pharmacological study, prompted us to isolate a gene encoding a putative PI-PLC from wild-type strain 70-15. Using polymerase chain reaction (PCR) amplification with degenerate primers (Jung *et al.*, 1997), we were able to identify *MoPLC1* (GenBank Accession Number AF098645) in the fungal genome. The *MoPLC1* gene contains no intron and encodes a long polypeptide of 847 amino acids. The predicted amino acid sequence shows high similarity to other fungal PLCs: 64% and 50% identity to those of *Botryotinia fuckeliana* BPLC1 (GenBank Accession Number U65685) and *Saccharomyces cerevisiae* PLC1 (GenBank Accession Number D38393) (Jung *et al.*, 1997, Yoko-o *et al.*, 1993), respectively. To date, only PLC-δ-related forms have been found in lower eukaryotes, such as yeast and slime moulds, suggesting an evolutionary relationship in which other subtypes in higher eukaryotes evolved from PLC-δ through duplication and divergence (Koyanagi *et al.*, 1998). Our analysis of domain architecture using deduced amino acid sequences showed that MoPLC1 is also most closely related to the mammalian PLC-δ subtype (Fig. 2A) (Rebecchi and Pentyala, 2000). MoPLC1 contains five domains common to PLC-δ: a pleckstrin homology (PH) domain, an EF-hand domain, conserved catalytic domains X and Y, and a C-2 domain. However, splice variants as found in mammalian *PLC-δ4* were not detected in our analysis of the *MoPLC1* transcript (data not shown).

To test the genetic link between *MoPLC1* and calcium flux, we performed targeted gene deletion by replacing *MoPLC1* with a gene encoding hygromycin phosphotransferase (*HPH*), and examined the calcium flux in the resulting mutant. The gene replacement vector (pRHOKO3) was constructed using genomic DNA from
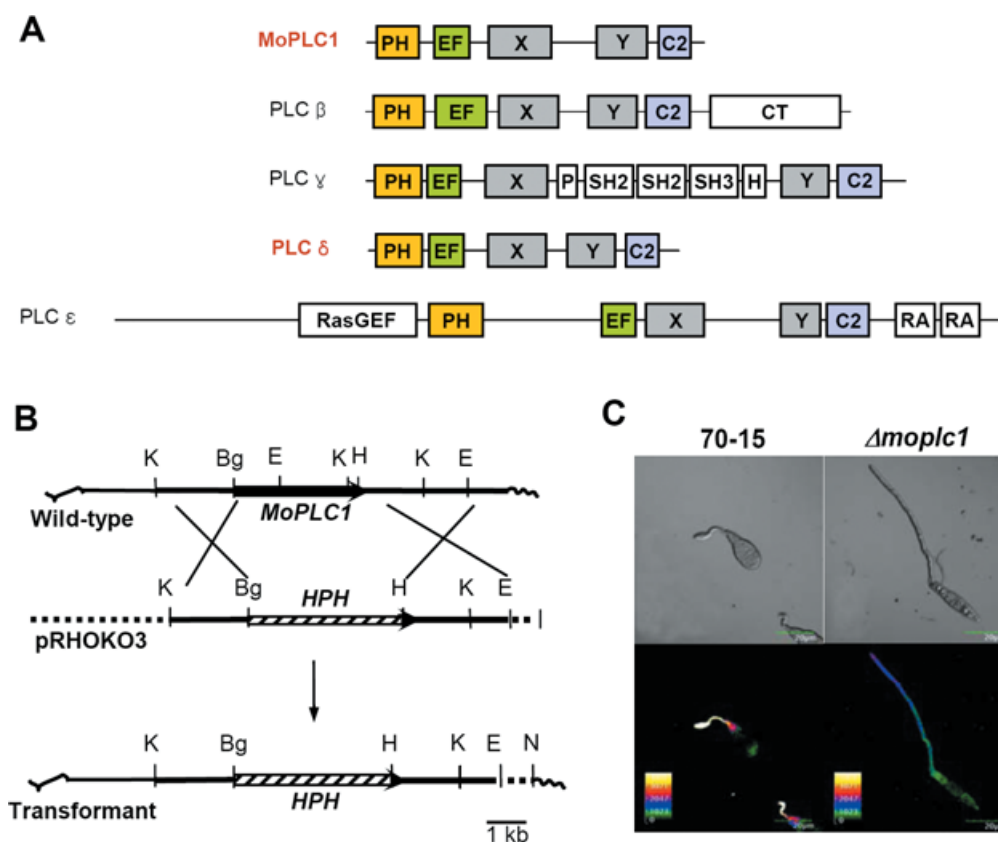

Fig. 2 Comparison of domain architecture between *Magnaporthe oryzae* phospholipase C 1 (MoPLC1) and mammalian phospholipase C (PLC) subtypes, and the effect of deletion of *MoPLC1* on calcium fluxes in the fungus. (A) Domain architecture of PLC subtypes. PH, pleckstrin homology domain; EF, EF-hand domain; X, catalytic X domain; Y, catalytic Y domain; C2, C2 domain; CT, regulatory carboxyl terminus; RasGEF, guanine nucleotide exchange factor domain for Ras-like small GTPases; RA, Ras association domain; SH, internal Src-homology domain. (B) Schematic diagram showing the strategy used for targeted deletion of the *MoPLC1* gene. K, *Kpn*I; Bg, *Bgl*II; H, *Hind*III; E, *Eco*RI; N, *Not*I. (C) Effect of *MoPLC1* deletion on calcium fluxes. Germinating conidia on a hydrophobic surface were photographed either under differential interference contrast microscopy (top panels) or confocal microscopy (bottom panels). C, conidium; G, germ tube. Scale bar, 20 μm.

regions flanking the *MoPLC1* gene, and then transformed into the wild-type strain (Fig. 2B). A deletion mutant (*Δmoplc1*) with the *MoPLC1* gene replaced by *HPH* via homologous recombination was selected, and the correct gene replacement event in *Δmoplc1* was confirmed by Southern blot analysis (Fig. S1, see Supporting Information). Imaging of $[Ca^{2+}]_{int}$ clearly showed that the calcium flux observed in the wild-type was suppressed by the deletion of *MoPLC1* (Fig. 2C), indicating that MoPLC1 is the modulator of calcium flux during infection-specific morphogenesis.

MoPLC1 is required for vegetative, asexual and sexual development

To elucidate the functions of MoPLC1-mediated calcium signalling in *M. oryzae*, we searched for possible phenotypes of the mutant. The *Δmoplc1* mutant showed a retarded growth rate on complete medium compared with that of the wild-type (Table 1), although the colony morphologies of both strains were indistinguishable. A similar growth defect was reported for a deletion mutant of the PLC gene (*Δcplc1*) in *Cryphonectria parasitica* (Chung *et al.*, 2006). It was demonstrated that the rate of hyphal extension in *Neurospora crassa* is dependent on calcium concentration, which, in turn, relies on the activation of stretch-activated PLC (Silverman-Gavrila and Lew, 2003). The growth retardation of *Δmoplc1* suggests a comparable role for MoPLC1-mediated calcium signalling in hyphal growth. In yeast, hyperosmotic shock can induce the release of internal Ca^{2+}, suggesting that calcium signalling is involved in osmo-sensing and regulation (Denis and Cyert, 2002). When the mutant and wild-type strains were grown on complete medium supplemented with 0.4 M sodium chloride or 1 M glycerol, mycelia of *Δmoplc1* underwent lysis under hypertonic conditions (Fig. 3A). This suggests that MoPLC1-mediated calcium signalling is also involved in cellular processes that counteract osmotic stress in *M. oryzae*.

Δmoplc1 produced a dramatically reduced number of conidia (asexual spores) with aberrant morphology (Table 1; Fig. 3B, top
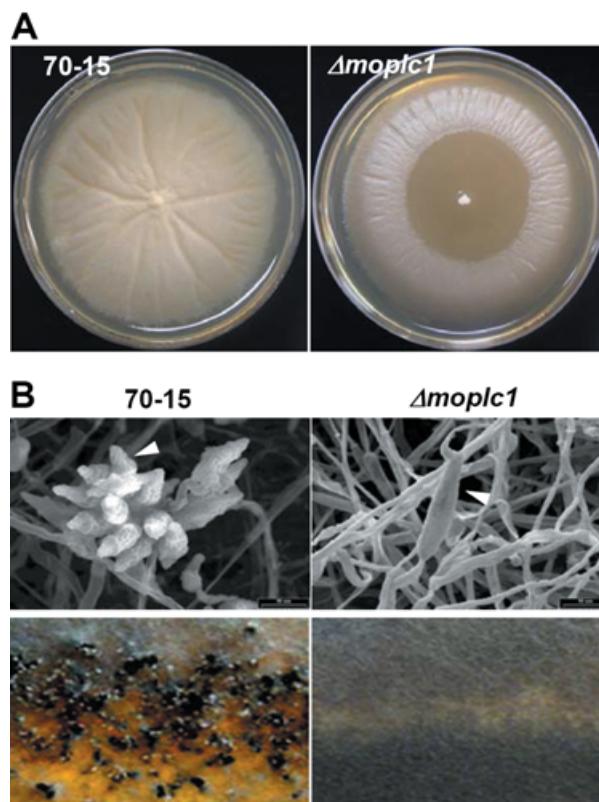

Fig. 3 Sensitivity to osmotic stress and defects in asexual and sexual reproduction of *Δmoplc1*. (A) Growth of the wild-type and *Δmoplc1* under hypertonic conditions. Wild-type and *Δmoplc1* were grown on complete medium supplemented with glycerol (1 M) or sodium chloride (0.4 M) to test their sensitivity to osmotic stress. (B) Defect of *Δmoplc1* in asexual and sexual reproduction. The conidial production of 70-15 and *Δmoplc1* was examined using scanning electron microscopy (top panels). The ability of sexual reproduction was tested by allowing each strain (MAT1-2) to grow facing the strain of opposite mating type (MAT1-1), 70-6, on oatmeal agar plates (bottom panels).

Table 1 Comparison of growth rate, conidiation, germination and appressorium formation among strains.

Strain	Growth (mm)*	Conidiation† (×10⁴ spores/mL)	Conidial germination (%)‡	Appressorium formation (%)§		
				12 h	24 h	48 h
70-15	54.7 ± 0.6	753	98.7 ± 0.6	92.0 ± 1.7	96.0 ± 1.7	95.0 ± 1.0
Δmoplc1	40.0 ± 3.5	428	95.0 ± 2.6	21.7 ± 1.6	38.3 ± 4.0	49.7 ± 4.2
NC-17	64.7 ± 2.5	695	98.0 ± 1.7	94.7 ± 1.6	94.3 ± 2.5	96.3 ± 1.2
IC-19	57.7 ± 2.1	497	97.7 ± 1.5	95.0 ± 2.0	98.3 ± 3.8	97.3 ± 1.2

*Growth was measured as the diameter of fungal mycelia grown on complete medium for 12 days.

†Conidiation was measured as the number of conidia in 1 mL of conidial suspension using a haemocytometer under a microscope. The conidial suspensions were prepared by flooding the 12-day-old fungal cultures grown on complete medium with 10 mL of sterilized distilled water.

‡Conidial germination was measured as the percentage of germinated conidia.

§Appressorium formation was measured as the percentage of appressorium formation among germinated conidia.
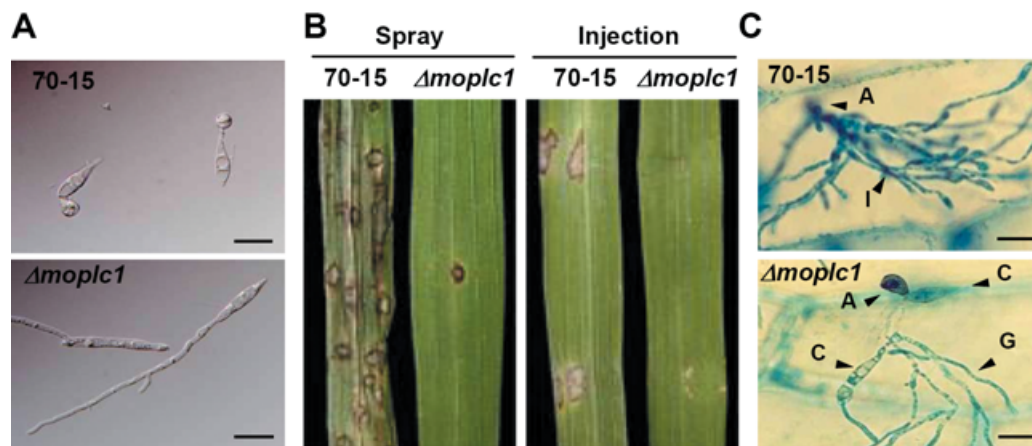
Fig. 4 Appressorium formation and pathogenicity of *Δmoplc1*. (A) Appressorium formation on a plastic coverslip as an inductive surface was compared between 70-15 and *Δmoplc1*. (B) Pathogenicity test. Conidial suspensions were either sprayed onto rice leaves or injected into plant tissues using a syringe for the pathogenicity assay. (C) Penetration defect of *Δmoplc1*. Ability to penetrate the plant cell was tested by placing the conidial suspension on onion epidermal cells. Scale bar, 20 μm.

panels). A close examination of the spore ontogeny revealed that the mutant produced one narrow and elongated conidium frequently having more than three cells on one conidiophore; in contrast, the wild-type produced pear-shaped, three-celled conidia borne in a sympodial pattern on a conidiophore (Fig. S2, see Supporting Information). When the mating proficiency of *Δmoplc1* (*MAT1-2*) mutant was tested by crossing it with the near-isogenic wild-type strain 70-6 (*MAT1-1*), the mutant failed to develop dark-pigmented perithecia in the border between the two strains (Fig. 3B, bottom panels).

MoPLC1 is required for appressorium development and pathogenicity

Appressorium formation of *Δmoplc1* on a hydrophobic surface showed severe defects (Fig. 4A). Conidia of *Δmoplc1* frequently produced long germ tubes with branches, and only about 20% of the germinated conidia formed boot-shaped appressoria after 12 h of incubation, whereas over 90% of the germinated conidia of the wild-type formed dome-shaped appressoria over a similar time frame (Table 1). The frequency of appressorium formation in *Δmoplc1* gradually increased to 49% after 48 h of incubation. These results are in accordance with our calcium imaging data, suggesting that MoPLC1-mediated calcium signalling is involved in surface sensing and appressorium morphogenesis. However, the delay, rather than incapacitation, of appressorium formation exhibited by *Δmoplc1* suggests that MoPLC1-mediated calcium signalling is necessary, but not sufficient, for complete differentiation of the appressorium. In addition, the defective appressorium formation in *Δmoplc1* could be significantly restored, but not to the wild-type level (96%), by exogenous calcium, DAG or a combination of the two (59%, 62% and 62%, respectively). This

partial remediation suggests that MoPLC1 is involved in various cellular signalling processes other than regulating the intracellular levels of calcium and DAG, and that the inhibition of MoPLC1 by neomycin might be incomplete.

To determine the role of MoPLC1-mediated calcium signalling in fungal pathogenicity, seedlings of the susceptible rice cultivar Nagdong were inoculated with a conidial suspension of the wild-type strain 70-15 or *Δmoplc1*. On this cultivar, *Δmoplc1* was nearly non-pathogenic, causing few lesions that failed to develop further, whereas the wild-type developed numerous typical spindle-shaped lesions that often coalesced with other lesions in close proximity (Fig. 4B, left panel). The pathogenicity defect of *Δmoplc1* cannot be fully accounted for by the marked reduction in appressorium formation. To further explain the pathogenicity defect of *Δmoplc1*, the invasive growth and penetration of the mutant were examined. When *Δmoplc1* conidia were injected into rice leaves to allow direct entry through the wound site, they failed to grow inside the host plant (Fig. 4B, right panel). In penetration assays using onion epidermal cells, most wild-type conidia formed appressoria that penetrated the epidermis and developed ramifying bulbous invasive hyphae (Fig. 4C, top panel). However, *Δmoplc1* conidia infrequently formed appressoria and failed to penetrate plant cells, and thus produced no invasive hyphae (Fig. 4C, bottom panel).

To test whether the inability of the mutant to penetrate plant cells resulted from insufficient turgor pressure within its appressoria, we performed incipient cytorrhysis assay using 1, 3 or 5 M glycerol solution (Howard *et al.*, 1991). Intriguingly, the proportion of collapsed appressoria remained almost constant in the mutants over all glycerol concentrations applied, whereas the collapse rate of wild-type appressoria increased as the concentration of glycerol solution increased (Fig. S3, see Supporting Information).
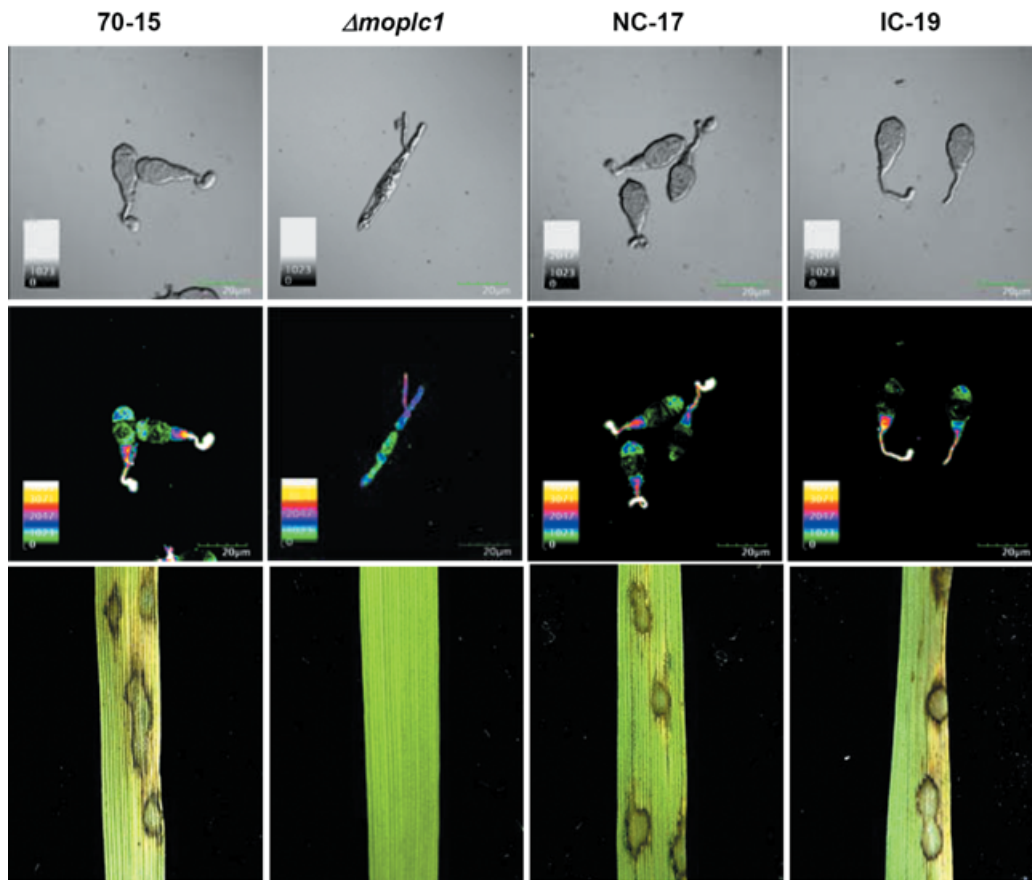
Fig. 5 Complementation of calcium fluxes and pathogenicity in Δ*moplc1* by the introduction of fungal and mammalian phospholipase C (PLC). The complementation for calcium fluxes and fungal pathogenicity in Δ*moplc1* by the introduction of either *Magnaporthe oryzae* phospholipase C 1 (*MoPLC1*) or mouse *PLC δ-1* is shown. The calcium fluxes at the tip of the germ tube were monitored and pathogenicity was tested for both complements: NC-17 (native complementation) and IC-19 (inter-kingdom complementation). Top and middle panels show the germinating conidia of each strain on a hydrophobic surface observed under differential interference contrast and confocal microscopy. Bottom panels show the pathogenicity of each strain on rice plants.

A similar observation was made in the study of a MAP kinase kinase kinase, *MCK1,* which was reported to play a pivotal role in maintaining cell wall integrity in *M. oryzae* (Jeon *et al.*, 2008). Our data suggest that MoPLC1 might also be involved in maintaining cell wall integrity through the regulation of the MAP kinase pathway. Taken together, we conclude that MoPLC1-mediated calcium signalling is involved in several aspects of disease causation and fungal life cycle completion on its host.

The phenotype of Δ*moplc1* is recovered by introduction of the *MoPLC1* gene

To ensure that the phenotypic changes observed in Δ*moplc1* were associated with the gene replacement event, we introduced a wild-type allele of the *MoPLC1* gene under the control of its native promoter (Fig. S4, see Supporting Information) into the *MoPLC1* deletion mutant by co-transformation with pII99 containing

a geneticin-resistance gene as a selectable marker. From the transformants produced, we selected the transformant, NC-17, which contains the *MoPLC1* gene in its genome (Fig. S5, see Supporting Information). Examination of NC-17 showed that the introduction of the *MoPLC1* gene into Δ*moplc1* could resurrect the cytoplasmic calcium flux (Fig. 5), thereby recovering all defects in the phenotype, including pathogenicity, to the wild-type level (Table 1; Fig. 5). We conclude that deletion of the *MoPLC1* gene is responsible for the suppression of the calcium flux that leads to diverse phenotypic changes in *M. oryzae*.

Mammalian PLC-δ functionally substitutes for MoPLC1

Our analysis of the deduced amino acid sequences indicated that MoPLC1 belongs to the δ type of PLC. In addition, the predicted three-dimensional structure of MoPLC1 shows remarkable similarity to the crystallographic structure of mouse PLC-δ1 (Essen

et al., 1996), notwithstanding the different lengths and low similarity of the two gene products (RASMOL program: http://www.umass.edu/microbio/rasmol/index2.htm). These findings led us to test whether mammalian PLC-δ could function in place of fungal PLC. As an inter-kingdom complementation experiment, we introduced the mouse *PLC-δ1* cDNA (Lee *et al.*, 1999) under the control of the *MoPLC1* promoter (Figs S4 and S5, see Supporting Information) into Δ*moplc1*. Surprisingly, imaging of cytoplasmic calcium in the representative transformant, IC-19, showed that mouse PLC-δ1 is able to induce calcium flux in *M. oryzae* (Fig. 5). This observation clearly demonstrates the functional conservation of PLC between two distinct kingdoms as a regulator of calcium signalling. Like the NC-17 strain, the IC-19 strain was able to grow normally, develop appressoria and cause disease lesions on rice leaves to the wild-type level (Table 1; Fig. 5). However, the conidiation of Δ*moplc1* was not fully restored by the introduction of mouse *PLC-δ1*. Although more information should be forthcoming on the biology of mammalian PLC-δ, it is conceivable that fungal PLC has unique regulatory and biological roles pertaining to kingdom-specific reproductive mechanisms that cannot be complemented by its mammalian counterparts.

CONCLUDING REMARKS

In this study, we have demonstrated that the PLC-mediated regulation of calcium flux is pivotal for the fungus to cause disease on its host, and this regulation is conserved across animal and fungal kingdoms. A recent comparative genomic analysis revealed that fungi do not possess components of calcium mobilization mechanisms from internal stores, as found in plants and animals, suggesting the existence of a fungal-specific mechanism that has yet to be identified (Zelter *et al.*, 2004). Considering the commonalities of fungal pathogenesis in plants and animals, a comparative study of the molecular mechanisms of calcium signalling in both fungal pathogens and their hosts would provide evolutionary insights into fungal pathogenesis and also novel strategies for the control and therapeutic treatment of costly and life-threatening fungal infections.

EXPERIMENTAL PROCEDURES

Strains and culture conditions

Magnaporthe oryzae strain 70-15 (MAT1-1) was provided by A. Ellingboe (University of Wisconsin, Madison, WI, USA), and used for the cloning and disruption of the *MoPLC1* gene. *Magnaporthe oryzae* strain 70-6, carrying the MAT1-2 mating type allele, was used to test for sexual reproduction ability. Fungal cultures were grown on oatmeal agar medium (OMA; 50 g oatmeal per litre) at 25 °C under constant fluorescent light to promote conidia formation.

Imaging of intracellular calcium of the fungus

The relative $[Ca^{2+}]_{int}$ was measured by imaging the emission intensities of the Ca^{2+}-sensitive fluorescent dyes calcium orange/AM (7 μM) and calcium green/AM (8 μM) (Molecular Probes, Eugene, OR, USA) for the imaging of the wild-type and comparison of the wild-type and mutants, respectively. Fluorescence imaging of Ca^{2+} in germinating conidia was performed using a Bio-Rad MRC-1024 confocal apparatus with a krypton–argon mixed gas laser attached to a Nikon Diaphot TMD inverted microscope (Bio-Rad Microscience, Hemel Hempstead, Hertfordshire, UK). The dye was excited at 488 and 530 nm using 5.1% laser intensity, and emitted fluorescence was detected at 500 and 600 nm. The germinating conidia of *M. oryzae* were observed using a 60×0.75 NA objective (digital factor, 2). Increases in $[Ca^{2+}]_{int}$ were expressed as a percentage of the observed to expected intensity of the total fluorescence of calcium indicator used.

Assays for appressorium formation and pathogenicity

Conidia germination and appressorium formation were assayed using GelBond film (FMC Bioproducts, Rockland, ME, USA) as an inductive surface. Conidia were harvested from 10-day-old cultures on OMA plates using sterile distilled water. A 40-μL aliquot of conidial suspension (3×10^4 or 4×10^4 conidia/mL) was spotted onto the inductive surface, and incubated in a moist box at 25 °C. The conidial germination and appressorium formation rates were measured by counting at least 100 conidia under a light microscope at 12, 24 and 48 h post-incubation. To test the effects of chemicals, 40 μL of conidial suspension was treated with 30 μM 1,2-dioctanoyl-*sn*-glycerol, 0.1 M $CaCl_2 \cdot 2H_2O$ or 0.1 M neomycin sulphate.

For pathogenicity assay, conidia were harvested from 10-day-old oatmeal agar cultures, and 10 mL of conidial suspension (3×10^5 conidia/mL) in 250 ppm Tween-20 was spray inoculated onto the leaves of 3-week-old rice seedlings (susceptible rice cv. Nakdong). Rice plants inoculated with conidia were incubated in a dew chamber at 25 °C in the dark. After 24 h, the rice plants were moved to a growth chamber with a photoperiod of 16 h light/8 h dark. Disease severity was rated 7 days after inoculation. For the infiltration infection assay, 100 μL of conidial suspension was wound inoculated into leaves of 3-week-old rice cv. Nakdong plants at three points per leaf. Disease severity was rated 5–7 days later.

DNA isolation and construction of the target gene replacement and complementation vectors

The *MoPLC1* gene was isolated using PCR with degenerate primers designed to hybridize with the conserved domains of

S. cerevisiae PLC1: SSHNTY (PLCX, 5′-CG*GAATTC*AGYTCN-CAYAAYACNTA-3′), containing a terminal *Eco*RI site in the X domain, and GYVLKP (PLCY, 5′-CG*GGATCC*GGYTTRAANACRTANCC-3′), containing a terminal *Bam*HI site in the Y domain. The PCR product was cloned into pUC19 (pPLCp) and used to screen a BAC library of *M. oryzae* 70-15 strain. BAC clones that hybridized with pPLCp were selected. Their DNA was digested and mapped with several restriction enzymes individually and in combination. The largest two fragments that hybridized with pPLCp were subcloned into pBluescript KS+. The nucleotide sequences of eight subclones (pRHO1–8) from pRHO01 and pRHO02 were determined using a BigDye DNA sequencing kit (Applied Biosystems, Foster City, CA, USA) on an ABI 377 DNA sequencer. Sequencing PCR was performed with BigDye mixture following the manufacturer's instructions. The *MoPLC1* gene replacement vector, pRHOKO3, was generated by a one-step ligation method with a 1.8-kb *Kpn*I and *Bgl*II fragment of pRHO02 containing the 5′-flanking region, a 2.2-kb *Hin*dIII and *Eco*RI fragment of pRHO01 containing the 3′-flanking region, and a 3.8-kb *Bgl*II and *Hin*dIII *Hph* cassette into pBluescript containing *Kpn*I and *Eco*RI ends by three-way ligation. pRHOKO3 was linearized with *Not*I and transformed into 70-15 strain. To complement the Δ*moplc1* mutant, a native complementation vector, pFunc1, was constructed by cloning a 3.0-kb *Kpn*I and *Sal*I fragment from pRHO02 containing the promoter region and open reading frame (ORF) and a 3.5-kb *Sal*I and *Pst*I fragment from pRHO01 containing the rest of the ORF and a terminator into pBluescript with *Kpn*I and *Pst*I ends by one-step ligation. pFunc1 was co-transformed with pII99 containing a geneticin-resistance cassette. After selection on TB3 containing geneticin, resistant transformants were identified by PCR with PLCX and PLCY and confirmed by Southern hybridization analysis. An inter-kingdom complementation vector, pFunc2, was generated by cloning a 1.5-kb *Kpn*I and *Xho*I fragment of a PCR product amplified using the primers PMF2 (5′-GGTACCCTAG-CAAGTCCAGATTGC-3′) and PMR1 (5′-CTCGAGGCTTGTTTTC-CGCGACAG-3′), containing the *MoPLC1* gene promoter region, into the pBP vector, which harbours the mPLCδ1 full-length cDNA between the *Hin*dIII and *Eco*RI sites. pFunc2 was also co-transformed with pII99 and positive transformants were selected on TB3 containing geneticin. Transformants for this complementation experiment were identified by PCR and Southern hybridization.

Database searches and computer analysis of the sequence

Searches for sequences showing homology at the DNA and protein levels were performed using the BLAST algorithm at the National Center for Biotechnology Information and European Bioinformatics Institute. For domain and secondary structure analysis, the ExPASY proteomics server (Geneva, Switzerland) was used. Domains were analysed using SMART (Simple Modular Architecture Research Tool; http://www.ebi.ac.uk/interpro) and Motif scan in protein sequence (ISREC Bioinformatics; http://hits.isb-sib.ch/cgi-bin/PFSCAN). Phylogenetic relationships were assessed using neighbour-joining methods with the Lasergene programs (DNAstar, Madison, WI, USA) and PAUP* version 4.0s (R2 Swofford, 2000).

REFERENCES

Ahn, I.P., Kim, S., Choi, W.B. and Lee, Y.H. (2003) Calcium restores prepenetration morphogenesis abolished by polyamines in *Colletotrichum gloeosporioides* infecting red pepper. *FEMS Microbiol. Lett.* **227**, 237–241.

Berridge, M.J., Bootman, M.D. and Lipp, P. (1998) Calcium—a life and death signal. *Nature*, **395**, 645–648.

Berridge, M.J., Bootman, M.D. and Roderick, H.L. (2003) Calcium signalling: dynamics, homeostasis and remodelling. *Nat. Rev. Mol. Cell Biol.* **4**, 517–529.

Chandra, S., Leinhos, G.M., Morrison, G.H. and Hoch, H.C. (1999) Imaging of total calcium in urediospore germlings of *Uromyces* by ion microscopy. *Fungal. Genet Biol.* **27**, 77–87.

Chung, H.J., Kim, M.J., Lim, J.Y., Park, S.M., Cha, B.J., Kim, Y.H., Yang, M.S. and Kim, D.H. (2006) A gene encoding phosphatidyl inositol-specific phospholipase C from *Cryphonectria parasitica* modulates the lac1 expression. *Fungal. Genet Biol.* **43**, 326–336.

Couch, B.C. and Kohn, L.M. (2002) A multilocus gene genealogy concordant with host preference indicates segregation of new species, *Magnaporthe oryzae* from *M. grisea*. *Mycologia*, **94**, 683–693.

Dean, R.A., Talbot, N.J., Ebbole, D.J., Farman, M.L., Mitchell, T.K., Orbach, M.J., Thon, M., Kulkarni, R., Xu, J.R., Pan, H., Read, N.D., Lee, Y.H., Carbone, I., Brown, D., Oh, Y.Y., Donofrio, N., Jeong, J.S., Soanes, D.M., Djonovic, S., Kolomiets, E., Rehmeyer, C., Li, W., Harding, M., Kim, S., Lebrun, M.H., Bohnert, H., Coughlan, S., Butler, J., Calvo, S., Ma, L.J., Nicol, R., Purcell, S., Nusbaum, C., Galagan, J.E. and Birren, B.W. (2005) The genome sequence of the rice blast fungus *Magnaporthe grisea*. *Nature*, **434**, 980–986.

Denis, V. and Cyert, M.S. (2002) Internal Ca(2+) release in yeast is triggered by hypertonic shock and mediated by a TRP channel homologue. *J. Cell Biol.* **156**, 29–34.

Essen, L.O., Perisic, O., Cheung, R., Katan, M. and Williams, R.L. (1996) Crystal structure of a mammalian phosphoinositide-specific phospholipase C delta. *Nature*, **380**, 595–602.

Goff, S.A., Ricke, D., Lan, T.H., Presting, G., Wang, R., Dunn, M., Glazebrook, J., Sessions, A., Oeller, P., Varma, H., Hadley, D., Hutchison, D., Martin, C., Katagiri, F., Lange, B.M., Moughamer, T., Xia, Y., Budworth, P., Zhong, J., Miguel, T., Paszkowski, U., Zhang, S., Colbert, M., Sun, W.L., Chen, L., Cooper, B., Park, S., Wood, T.C., Mao, L., Quail, P., Wing, R., Dean, R., Yu, Y., Zharkikh, A., Shen, R., Sahasrabudhe, S., Thomas, A., Cannings, R., Gutin, A., Pruss, D., Reid, J., Tavtigian, S., Mitchell, J., Eldredge, G., Scholl, T., Miller, R.M., Bhatnagar, S., Adey, N., Rubano, T., Tusneem, N., Robinson, R., Feldhaus, J., Macalma, T., Oliphant, A. and Briggs, S. (2002) A draft sequence of the rice genome (*Oryza sativa* L. ssp. japonica). *Science*, **296**, 92–100.

Hoch, H.C., Staples, R.C. and Bourett, T. (1987) Chemically induced appressoria in *Uromyces appendiculatus* are formed aerially, apart from the substrate *Mycologia*, **79**, 418–424.

Howard, R.J., Ferrari, M.A., Roach, D.H. and Money, N.P. (1991) Penetration of hard substrates by a fungus employing enormous turgor pressures. *Proc. Natl. Acad. Sci. USA*, **88**, 11 281–11 284.

Idnurm, A., Bahn, Y.S., Nielsen, K., Lin, X., Fraser, J.A. and Heitman, J. (2005) Deciphering the model pathogenic fungus *Cryptococcus neoformans*. *Nat. Rev. Microbiol.* **3**, 753–764.

Jeon, J., Goh, J., Yoo, S., Chi, M.H., Choi, J., Rho, H.S., Park, J., Han, S.S., Kim, B.R., Park, S.Y., Kim, S. and Lee, Y.H. (2008) A putative MAP kinase kinase kinase, MCK1, is required for cell wall integrity and pathogenicity of the rice blast fungus, *Magnaporthe oryzae. Mol. Plant–Microbe. Interact.* **21**, 525–534.

Jeon, J., Park, S.Y., Chi, M.H., Choi, J., Park, J., Rho, H.S., Kim, S., Goh, J., Yoo, S., Choi, J., Park, J.Y., Yi, M., Yang, S., Kwon, M.J., Han, S.S., Kim, B.R., Khang, C.H., Park, B., Lim, S.E., Jung, K., Kong, S., Karunakaran, M., Oh, H.S., Kim, H., Kim, S., Park, J., Kang, S., Choi, W.B., Kang, S. and Lee, Y.H. (2007) Genome-wide functional analysis of pathogenicity genes in the rice blast fungus. *Nat. Genet.* **39**, 561–565.

Jung, O.J., Lee, E.J., Kim, J.W., Chung, Y.R. and Lee, C.W. (1997) Identification of putative phosphoinositide-specific phospholipase C genes in filamentous fungi. *Mol. Cells* **7**, 192–199.

Kankanala, P., Czymmek, K. and Valent, B. (2007) Roles for rice membrane dynamics and plasmodesmata during biotrophic invasion by the blast fungus. *Plant Cell* **19**, 706–724.

Koyanagi, M., Ono, K., Suga, H., Iwabe, N. and Miyata, T. (1998) Phospholipase C cDNAs from sponge and hydra: antiquity of genes involved in the inositol phospholipid signaling pathway. *FEBS Lett.* **439**, 66–70.

Lee, S.C. and Lee, Y.H. (1998) Calcium/calmodulin-dependent signaling for appressorium formation in the plant pathogenic fungus *Magnaporthe grisea. Mol Cells*, **8**, 698–704.

Lee, W.K., Kim, J.K., Seo, M.S., Cha, J.H., Lee, K.J., Rha, H.K., Min, D.S., Jo, Y.H. and Lee, K.H. (1999) Molecular cloning and expression analysis of a mouse phospholipase C-delta1. *Biochem. Biophys. Res. Commun*, **261**, 393–399.

Lee, Y.H. and Dean, R.A. (1993) cAMP regulates infection structure formation in the plant pathogenic fungus *Magnaporthe grisea. Plant Cell* **5**, 693–700.

Lee, Y.H. and Dean, R.A. (1994) Hydrophobicity of contact surface induces appressorium formation in *Magnaporthe grisea. FEMS Microbiol. Lett.* **115**, 71–76.

Lengeler, K.B., Davidson, R.C., D'Souza, C., Harashima, T., Shen, W.C., Wang, P., Pan, X., Waugh, M. and Heitman, J. (2000) Signal transduction cascades regulating fungal development and virulence. *Microbiol. Mol. Biol. Rev.* **64**, 746–785.

Odds, F.C., Gow, N.A. and Brown, A.J. (2001) Fungal virulence studies come of age. *Genome Biol*, **2**, reviews1009.1-1009.4 (doi:10.1186/gb-2001-2-3-reviews1009).

Rebecchi, M.J. and Pentyala, S.N. (2000) Structure, function, and control of phosphoinositide-specific phospholipase C. *Physiol. Rev.* **80**, 1291–1335.

Rhee, S.G. and Bae, Y.S. (1997) Regulation of phosphoinositide-specific phospholipase C isozymes. *J. Biol. Chem.* **272**, 15 045–15 048.

Sexton, A.C. and Howlett, B.J. (2006) Parallels in fungal pathogenesis on plant and animal hosts. *Eukaryot. Cell* **5**, 1941–1949.

Shaw, B.D. and Hoch, H.C. (2000) Ca^{2+} regulation of *Phyllosticta ampelicida* pycnidiospore germination and appressorium formation. *Fungal. Genet. Biol.* **31**, 43–53.

Silverman-Gavrila, L.B. and Lew, R.R. (2003) Calcium gradient dependence of *Neurospora crassa* hyphal growth. *Microbiology*, **149**, 2475–2485.

Talbot, N.J. (2003) On the trail of a cereal killer: exploring the biology of *Magnaporthe grisea. Annu. Rev. Microbiol.* **57**, 177–202.

Yoko-o, T., Matsui, Y., Yagisawa, H., Nojima, H., Uno, I. and Toh-e, A. (1993) The putative phosphoinositide-specific phospholipase C gene, *PLC1*, of the yeast *Saccharomyces cerevisiae* is important for cell growth. *Proc. Natl. Acad Sci. USA*, **90**, 1804–1808.

Yu, J., Wang, J., Lin, W., Li, S., Li, H., Zhou, J., Ni, P., Dong, W., Hu, S., Zeng, C., Zhang, J., Zhang, Y., Li, R., Xu, Z., Li, S., Li, X., Zheng, H., Cong, L., Lin, L., Yin, J., Geng, J., Li, G., Shi, J., Liu, J., Lv, H., Li, J., Wang, J., Deng, Y., Ran, L., Shi, X., Wang, X., Wu, Q., Li, C., Ren, X., Wang, J., Wang, X., Li, D., Liu, D., Zhang, X., Ji, Z., Zhao, W., Sun, Y., Zhang, Z., Bao, J., Han, Y., Dong, L., Ji, J., Chen, P., Wu, S., Liu, J., Xiao, Y., Bu, D., Tan, J., Yang, L., Ye, C., Zhang, J., Xu, J., Zhou, Y., Yu, Y., Zhang, B., Zhuang, S., Wei, H., Liu, B., Lei, M., Yu, H., Li, Y., Xu, H., Wei, S., He, X., Fang, L., Zhang, Z., Zhang, Y., Huang, X., Su, Z., Tong, W., Li, J., Tong, Z., Li, S., Ye, J., Wang, L., Fang, L., Lei, T., Chen, C., Chen, H., Xu, Z., Li, H., Huang, H., Zhang, F., Xu, H., Li, N., Zhao, C., Li, S., Dong, L., Huang, Y., Li, L., Xi, Y., Qi, Q., Li, W., Zhang, B., Hu, W., Zhang, Y., Tian, X., Jiao, Y., Liang, X., Jin, J., Gao, L., Zheng, W., Hao, B., Liu, S., Wang, W., Yuan, L., Cao, M., McDermott, J., Samudrala, R., Wang, J., Wong, G.K. and Yang, H. (2005) The genomes of *Oryza sativa*: a history of duplications. *PLoS Biol.* **3**, e38.

Zeigler, R.S., Leong, S.A. and Teeng, P.S. (1994) *Rice Blast Disease*. Wallingford: CAB International.

Zelter, A., Bencina, M., Bowman, B.J., Yarden, O. and Read, N.D. (2004) A comparative genomic analysis of the calcium signaling machinery in *Neurospora crassa, Magnaporthe grisea*, and *Saccharomyces cerevisiae. Fungal. Genet. Biol.* **41**, 827–841.

SUPPORTING INFORMATION

Additional Supporting Information may be found in the online version of this article:

Fig. S1 Southern blot analysis of the mutants. Genomic DNA isolated from wild-type strain 70-15 (lane 1), *Δmoplc1* (lane 2) and ectopic transformants I-17 and II-35 (lanes 3 and 4) was digested with *Kpn*I. The blot was probed with *Kpn*I fragment from pRHOKO3. As expected, *Δmoplc1* exhibited the only 8.2-kb band and showed no hybridization at the 4.5-kb position.

Fig. S2 Conidiophore development and conidia formation of 70-15 and *∆moplc1* strains. Top panels show the density of conidiophores on which conidia are borne under a scanning electron microscope (×750). Bottom panels show the formation of conidia from a conidiophore observed under a light microscope (×400). The 70-15 strain forms conidia in a sympodial pattern on a conidiophore, whereas the conidia formation of *∆moplc* was not terminated after the formation of a conidium with three cells, producing an elongated conidium. Bar, 20 μm.

Fig. S3 Incipient cytorrhysis assay using 1, 3 and 5 M glycerol solution. For each glycerol concentration, at least 100 appressoria were observed, and the number of collapsed appressoria was counted from three independent experiments.

Fig. S4 Complementation vectors for the introduction of *MoPLC1* (A) and mouse *PLC δ-1* (B) into *∆moplc1*. Pmoplc1, promoter of *MoPLC1*; *ori*, origin of replication; Tmoplc1, terminator of *MoPLC1*; *Amp*[R], ampicillin resistance gene.

Fig. S5 Polymerase chain reaction (PCR)-based screening of transformants having *MoPLC1* and mouse *PLC δ-1* inserted *in trans* into the genome of *∆moplc1*. (A–D) Diagrams depicting the location of primers designed to screen the mutants and complements. NC, native complementation; IC, inter-kingdom complementation. (E) PCR was performed for genomic DNAs of each strain using either fungal-specific primers (PMF2 and PMR1) annealing to flanking regions of the *MoPLC1* gene, or a combination of fungal and mouse *PLC δ-1*-specific primers (PMF2 and MPR1) (Fig. S4). Lanes 1–4, 70-15, *∆moplc1*, NC-17 and IC-19 amplified with PMR2 and PMR1; lane 5, IC-19 amplified with PMF2 and MPR1; lane 6, pRHO15 as a positive control of IC transformants amplified with PMF2 and MPR1.

Please note: Wiley-Blackwell are not responsible for the content or functionality of any supporting materials supplied by the authors. Any queries (other than missing material) should be directed to the corresponding author for the article.